23rd International Conference on Renewable Energies and Power Quality (ICREPQ'25)
Tenerife (Spain), 25th to 27th June 20245
Renewable Energy and Power Quality Journal (RE&PQJ)
ISSN 2172-038 X, Volume No.23, September 2025

Dynamic Energy Management System for Optimal Energy Dispatch in a Microgrid Cluster

D. Carrasco-González[1], R. Sarrias-Mena[2], P. Horrillo-Quintero[1], F. Llorens-Iborra[1], I. De la Cruz-Loredo[3], C. E. Ugalde-Loo[3] and L. M. Fernández-Ramírez[1]

[1] Department of Electrical Engineering
Higher School of Engineering of Algeciras (ETSI Algeciras), University of Cádiz
Avda. Ramón Puyol, s/n – Algeciras, 11202 (Spain)

[2] Department of Engineering in Automation, Electronics, Computer Architecture & Networks
Higher School of Engineering of Algeciras (ETSI Algeciras), University of Cádiz
Avda. Ramón Puyol, s/n – Algeciras, 11202 (Spain)

[3] Centre for Integrated Renewable Energy Generation and Supply (CIREGS)
School of Engineering, Cardiff University
Cardiff, Wales, CF24 3AA (United Kingdom)

Abstract. Microgrid clusters (MGCs) have the ability to enhance energy efficiency, resilience, and reliability of individual microgrids (MGs). By integrating different power generation, consumption, and storage technologies, MGCs can combine direct current (DC) and alternating current (AC) technologies, thus offering flexibility to MGs. However, suitable control systems for MGCs are required to manage their operation, ensuring robustness and efficiency of the power dispatch. This work contributes to this effort by presenting and implementing a novel control approach for an MGC. The MGC consists of DC and AC MGs connected to a local electricity grid. The DC MG integrates a wind turbine, fuel cell, an electrolyzer, an ultracapacitor, and DC loads. In contrast, the AC MG integrates an electric battery bank, a photovoltaic generator and AC loads. The control system uses local controllers for each device in the cluster and a dynamic centralized energy management system to coordinate optimally energy dispatch and distribution among all energy storage systems. To assess the control approach, fluctuating incident solar radiation and winds speed, and dynamic loads conditions are introduced in the system. The control system demonstrates robust behavior across the different simulation scenarios.

Key words. Energy management system, microgrid cluster, sequence quadratic programming algorithm.

Abbreviations

AC	Alternating current
BESS	Battery energy storage system
DC	Direct current
EMS	Energy management system
ESS	Energy storage system
EZ	Electrolyzer
FC	Fuel cell
MG	Microgrid
MGC	Microgrid cluster
MPPT	Maximum power point tracking
P&O	Perturb and observe
PCC	Point of common coupling
PI	Proportional-integral
PV	Photovoltaic
RET	Renewable energy technology
SOC	State-of-charge
SQP	Sequence quadratic programming
UC	Ultra-capacitor
VSI	Voltage source inverter
WT	Wind turbine

1. Introduction

In recent years, the need to mitigate climate change has significantly increased the deployment of renewable power sources for energy production. This situation was generated by the international agreements to decarbonize the energy sector by mitigating greenhouse gas emissions and phasing out fossil fuels—primary drivers of climate change [1]. Moreover, energy demand in cities and industries is growing significantly. One possible response to these challenges is the development of smaller and more autonomous grids, known as microgrids (MGs). MGs offer advantages in terms of their reduced carbon emissions, improved energy quality and reliability, economic operation, and increased energy efficiency [2].

MGs combine distributed loads, energy storage systems (ESSs), and renewable energy technologies (RETs) into controlled, self-contained units with defined electrical limits [3]. Research efforts have primarily focused on alternating current (AC) MGs owing to their similarities with conventional grids. However, there has been recently an increased interest in direct current (DC) MGs [4]. This

has allowed MGs to operate using AC, DC, or a hybrid DC/AC configuration, enabling greater adaptability and flexibility [5].

MGs offer flexibility in operation, enabling them to function independently in remote regions where connecting to the main grid is difficult, as analyzed in [6]. However, MGs are often linked to the electricity grid via a point of common coupling (PCC). This connection enables two operational modes. In an island mode, the MG operates isolated from a main grid, relying solely on its internal generation and stored energy to meet local demand. Any excess or deficit in power needs to be managed within the MG using its RETs or ESSs [7]. In contrast, in a grid-connected mode, the MG interacts with the main grid, exchanging power as needed. The grid can supply additional power during periods of high demand within the MG or absorb excess power generated within the MG [8].

A natural step from integrating DC and AC technologies and connecting MGs to a conventional electricity grid is to interconnect several adjacent MGs as a microgrid cluster (MGC). This type of system offers several advantages: enhanced overall performance, including increased resilience, efficiency, reliability, and sustainability; localized energy balance, improving grid stability and self-sufficiency of a community; and decentralized power systems, reducing reliance in conventional electricity grids and promoting local energy autonomy [9].

Within the context of MG management, energy management systems (EMSs) are normally adopted to achieve operational goals. The main function of an EMS is the provision of reference signals for the constituent sources of the MG. Such a process may be implemented via diverse methodologies [10], [11]. However, in many cases, the EMS has been deployed for static systems with pre-established strategies, neglecting dynamic operational changes, such as fluctuations in demand or renewable energy generation [10]. In the case of [11], most of the developed EMS were applied to individual MGs, although coordinated control strategies among multiple MGs are increasingly emerging.

In this context, this work introduces a novel control approach for an MGC consisting of a DC MG and an AC MG linked to a local grid. The control system uses local controllers for each device and a dynamic centralized EMS that coordinates optimal power dispatch within the MGC based on a sequence quadratic programming (SQP) algorithm.

The remaining content of the paper is organized as follows. Section 2 describes the MGC configuration studied in this work. Section 3 describes the control system designed to manage the MGC operation. Section 4 shows and analyzes results obtained from different simulation scenarios, such as fluctuating incident solar radiation and winds speed, and dynamic loads conditions. Finally, conclusions are presented in Section 5.

2. Microgrid Cluster Configuration

The MGC configuration incorporates an AC MG, a DC MG, and a connection point with a local electricity grid, as shown in Fig. 1. A detailed specification of each element of the system is presented in the next subsections.

A. AC Microgrid

The AC MG comprises a solar photovoltaic (PV) power plant, local AC loads and an electric battery bank. All these devices are interconnected via a three-phase AC bus. This AC bus is also interconnected with the DC MG and the local electricity grid through a PCC. This configuration as a whole constitutes the MGC.

The PV generator was modelled with series and parallel resistances, a parallel diode model and a common current source [12]. The PV modules need a DC/DC boost converter to increase their voltage by implementing a maximum power point tracking (MPPT) strategy for

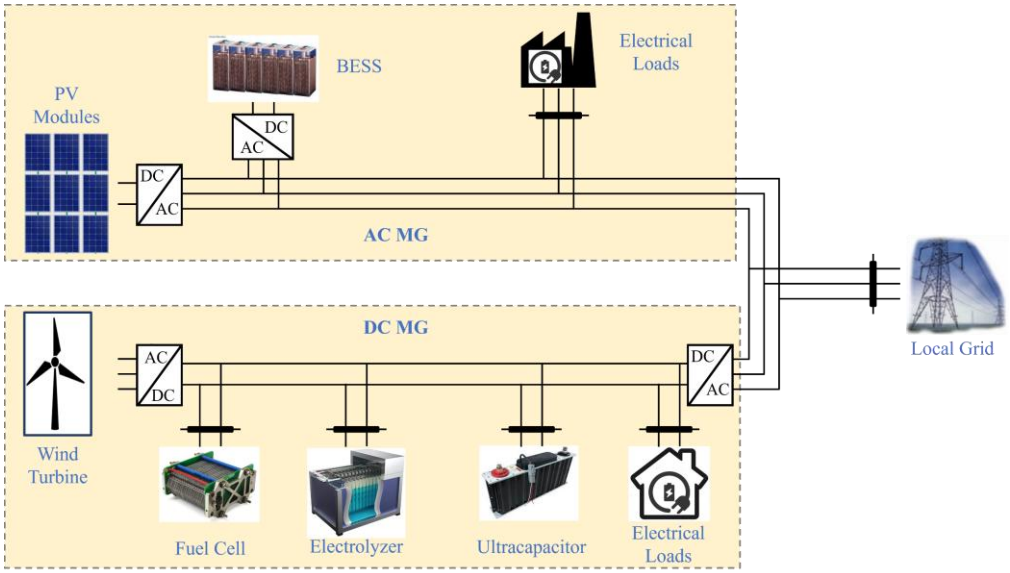

Fig. 1. Configuration of the MGC.

optimal power generation. The perturb and observe **(**P&O) method is used to determine the boost converter duty cycle, maximizing the PV output. A voltage source inverter (VSI) ensures compatibility with the local electricity grid by controlling voltage and frequency. The inverter incorporates cascaded control loops, employing proportional-integral (PI) controllers to maintain a constant DC output voltage of the boost converter [13].

The AC MG also incorporates a Li-ion battery energy storage system (BESS). The BESS is modelled as a series resistor with a controlled voltage source, reproducing its electrical characteristic. The BESS is connected to the AC bus voltage via a VSI. Employing cascaded control loops, the VSI regulates the reactive and active power exchange between the rest of the MG and the BESS.

Two local three-phase inductive loads connected in a star configuration are employed. These loads are dynamically disconnected and connected across different time periods to emulate fluctuating energy demand within the AC MG.

B. DC Microgrid

The DC MG consists of an ultra-capacitor (UC), a wind turbine (WT), hydrogen-based technologies including a fuel cell (FC) and an electrolyzer (EZ), and two local DC loads. All are linked via a DC bus, as illustrated in Fig. 1.

A WT based on a synchronous generator is considered in this study, modelled as a sixth-order system [14]. This generator is connected to the DC bus through an uncontrolled bridge rectifier that converts the generated AC power into DC, and a DC/DC boost converter that adapts the DC voltage levels and regulates the WT speed, optimizing the WT operation under fluctuating wind speeds.

With regards to the ESSs, a bidirectional half-bridge converter connected to the UC enables discharging and charging the UC, and thus a two-way energy exchange. Due to the unidirectional consumption nature of the EZ, a buck converter facilitates connection of the EZ to the DC bus. Conversely, a boost converter is essential for the FC owing to its unidirectional energy exchange capability, only allowing it to inject energy into the DC bus. The UC is represented by a series resistor with an ideal capacitor. The FC is represented by a diode model and a controlled voltage source. The EZ is modeled as a series resistance and a voltage source.

The local DC loads are directly connected to this MG. A controlled circuit breaker enables their connection and disconnection.

A VSI acts as the interface between the DC and AC buses. The purpose of this device is to convert DC power into AC power compatible with the AC MG, ensuring a stable DC bus voltage despite power variations arising from the variable wind speed and changing loads within the DC MG.

C. Local Grid

The MGC connects to a stable AC local grid represented by a three-phase voltage source with no internal impedance and constant voltage and frequency. This local grid is linked into the MGC via a PCC. Since the frequency and voltage at the PCC are self-adapted by the local grid, no specific control actions are necessary, as reactive and active energy exchange with this local grid are inherently controlled to maintain energy balance and prevent frequency and voltage fluctuations. For the current study, the MGC operates exclusively connected to the local grid, excluding the analysis of islanded operation.

3. Control Approach

This section summarizes the control approach implemented within the MGC. All elements of the MGC including RETs and ESSs are regulated independently to track a defined reference. At a higher layer, a dynamic centralized EMS oversees the entire MGC, orchestrating the optimal operation of all elements of the MGC. To this end, the SQP algorithm is adopted to solve the optimization problem to operate the MGC.

A. Local Control

This section summarizes the local control strategies implemented within the MGC to manage individual power converters and energy devices.

For the PV power plant, the P&O algorithm is utilized to execute the MPPT strategy and optimize power generation and dispatch under varying solar irradiance. Similarly, the WT speed is regulated to track the optimal power characteristic based on the wind speed.

The active power transfer among each ESS and the MGC is regulated by PI controllers, which control the active power to follow the reference values produced by the EMS. The UC controller accepts both negative and positive references, enabling both charging and discharging operations. The EZ controller only accepts negative references, corresponding to power consumption. Conversely, the FC controller only accepts positive references, implying power injection into the system.

Finally, time-controlled circuit breakers manage the connection/disconnection of DC and AC loads within each MG. The loads do not require dedicated control strategies since their behavior is already considered in the dynamic centralized EMS.

B. Optimal Energy Management System

A dynamic, optimal and centralized EMS, based on the SQP algorithm, was developed to regulate the operation of all elements of the MGC. In this sense, the EMS defines the different power references for all ESSs that form the MGC, with the objective of minimizing the reliance on the local electricity grid and ensuring the safety of the ESSs by monitoring their state-of-charge (SOC).

The centralized EMS is selected due to its advantages compared to a decentralized alternative. These advantages include reduced operational costs through optimized resource allocation across the MGC, simplified control and maintenance owing to less complex individual components, and enhanced efficiency through coordinated use of the diverse resources of the MGC [15].

Based on the previous assumptions, the primary function of the optimal EMS is to ensure energy balance by controlling the ESSs. This is accomplished by optimizing the energy exchange of the MGC with the local electricity grid. Three main inputs are required by the EMS: the SOC of the BESS, the total power generation P_{GEN}, given by the summation of individual power production of the RETs, and the total power demand P_{CON}, given by the summation of individual power demands in the MGC. The objective function of the optimization is:

$$min = \left\{ OF = \left| \left(P_{BESS_r} + P_{FC_r} + P_{EZ_r} \right) + \left(P_{GEN} - P_{CON} \right) \right|^2 \right\} \quad (1)$$

where P_{BESS_r}, P_{FC_r}, P_{EZ_r} denote the outputs of the optimization algorithm and represent the active power reference of the BESS, FC and EZ.

The EMS also considers the SOC of the BESS for energy storage or release as well as the power limits of the hydrogen system. Thus, the control algorithm may constrain these actions of different manners. In this paper, these security limitations are defined in the power constraints of the algorithm.

The BESS power constraints are $\left[-1 \cdot 10^6 + 1 \cdot 10^6 \cdot \left(\frac{SOC}{100} \right) W, 1 \cdot 10^6 \cdot \left(\frac{SOC}{100} \right) W \right]$. These constraints enable the device to charge or discharge based on its monitored SOC and ensure the safety operation of the BESS.

For the hydrogen system, power constraints are fixed depending on the maximum power outputs. The minimum power outputs are fixed based on a minimum power generation/consumption regime to avoid full disconnection when the devices are not required. Specifically, the power constraints of the hydrogen system are $[100\ W, 1.5 \cdot 10^6\ W]$ for the FC and $[-1 \cdot 10^6\ W, 100\ W]$ for the EZ.

The UC is used to handle transient power mismatches which the other ESSs cannot address due to their slower response. The active power refence of the UC (P_{UC_r}) is determined in as the deviation of the actual power output of the BESS, FC, and EZ (P_{BESS}, P_{FC}, and P_{Ez}) from their respective reference values. This is mathematically expressed as

$$P_{UC_r} = \left(P_{BESS_r} - P_{BESS} \right) + \left(P_{FC_r} - P_{FC} \right) + \left(P_{EZ_r} - P_{EZ} \right) \quad (2)$$

4. Simulation Results

To assess the performance of the control approach designed for the MGC, 10-second simulations were performed in MATLAB/Simulink. Different scenarios were modeled, consisting of fluctuating incident solar radiation (0.5 kW/m^2 for 1.5 s, 0.1 kW/m^2 from 1.5 to 3.5 s, and 0.9 kW/m^2 from 3.5 to 10 s) and wind speeds (15 m/s mean for the first 5 s, then 12.5 m/s) to mimic variations in PV and WT power generation. In addition, both AC and DC local loads were dynamically connected and disconnected. The DC loads, initially disconnected, include a 700 kW load that connects at 2.5 s and a 250 kW load that connects at 7.5 s. The AC local loads include a 1.8 MW/200 kVAr load, that remains constantly connected, and a 525 kW/100 kVAr load, that is alternately connected. The second load is connected between 1.5 s and 3 s, and again between 5 s and 10 s. Finally, the initial SoC of the BESS is 60%. All these conditions allow testing the dynamic behavior of the control system and the MGC.

Fig. 2 presents the power exchange with the local electricity grid ($\boldsymbol{P_{PCC}}$) and the generated and consumed power in the MGC. As shown in the figure, the local grid interacts with the MGC to maintain energy balance when there are changes in the inputs of the technologies comprised by the MGC. In addition, the local grid supplies or absorbs the difference in energy that the ESSs cannot handle to maintain the power balance. When generation and demand are balanced, the power exchange with the local grid decreases to a negligible level. Therefore, the optimal EMS minimizes the reliance on the local grid.

The variations in PV and WT power generation observed in Fig. 2 are caused by the fluctuations in the incident solar radiation and wind speed. Additionally, variations in the AC and DC local loads are caused by the connection/ disconnection of them into the AC and DC buses.

While both AC and DC local loads are modeled as constant values, the DC load profile exhibits minor fluctuations. These variations in the DC local loads are produced by the voltage fluctuations in the DC bus. The AC load profile does not exhibit this effect because the local grid ensures a steady voltage on the AC bus. A similar situation occurs with the WT power generation.

Fig. 3 shows the difference between the generated and consumed power in the MGC. This comparison enables understanding the MGC behavior when the ESSs are not

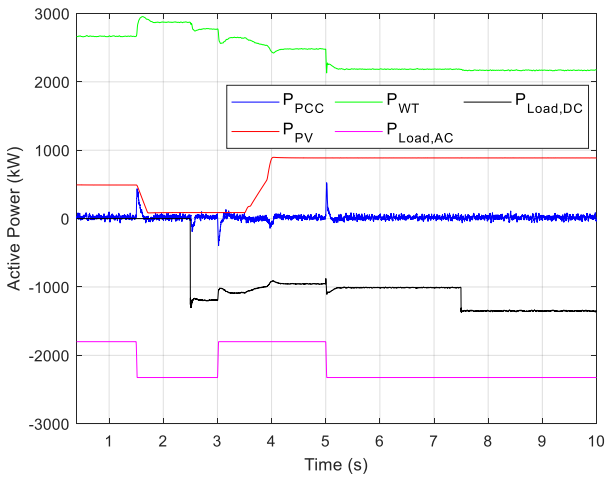

Fig. 2. Power exchange with the local grid (P_{PCC}) and the generated and consumed power in the MGC.

used to balance power. While the total generated power exceeds the total consumed power in the intervals 0-2.5 s and 3.5-5 s, the consumed power exceeds the generated powers in the rest of intervals of the simulation. This confirms the correct operation of the EMS to minimize the reliance of the system on the local electricity grid under the different power mismatches.

Fig. 4 shows the active power output of each ESS in the MGC and their corresponding references values. The results show that all technologies follow their respective references, which confirms the effectiveness of their controllers.

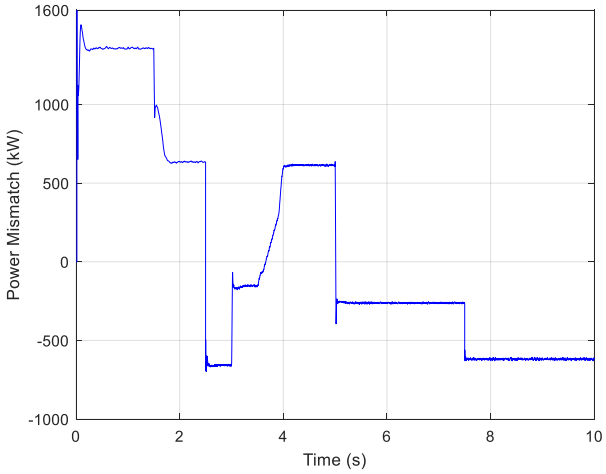

Fig. 3. Difference among the generated and consumed power in the MGC.

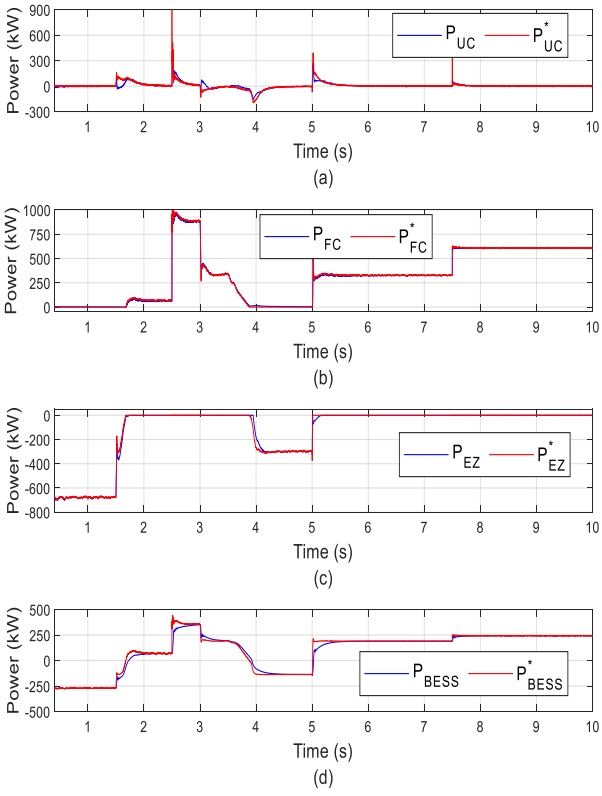

Fig. 4. Active power output of each ESS and their references: (a) UC, (b) FC, (c) EZ, and (d) BESS.

When the generated power exceeds the consumed power, the EMS directs the ESSs to store the excess energy. Conversely, when the consumed powers exceed the generated power, the EMS directs the ESSs to discharge energy into the MGC.

As the SOC of the BESS is near 60%, this device can store or supply energy at around half of its rated power. Additionally, the hydrogen technologies assist the BESS to maintain power balance in the system and ensure its adequate usage. As seen in the results in Fig. 4, the hydrogen system generated/consumed powers never reach the power bounds fixed in the algorithm.

In the last stage, the UC is able to handle transient power mismatches with large peaks. When the other ESSs reach a steady state, its power output returns near to zero.

Fig. 5 presents the voltage of the DC bus within the DC MG. This voltage is effectively controlled around its 1100 V reference value, which is crucial for the correct operation of all DC MG technologies. While changes in the hydrogen system and UC operation, DC local loads disconnection/connection, and WT production caused voltage fluctuations, the local control of the VSI of the DC MG controls effectively the voltage of the DC bus, maintaining it at the desired 1100 V reference.

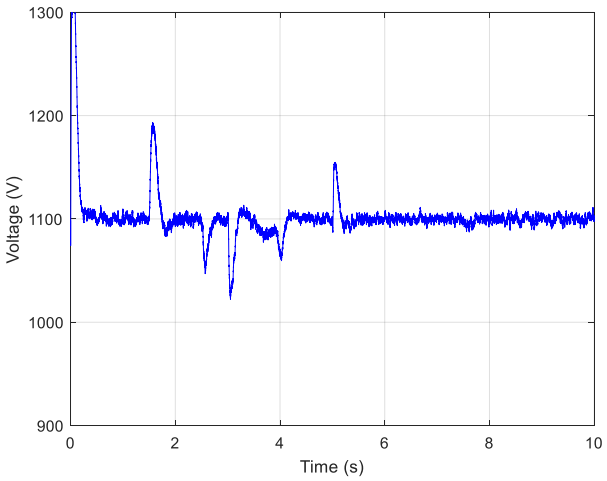

Fig. 5. Voltage of the DC bus profile.

The results presented in this section exhibit robust behavior across the different simulated scenarios and a satisfactory performance of the control system and the MGC.

5. Conclusion

This paper presented a novel control approach for an MGC comprising a DC MG and an AC MG connected to a local electricity grid. The system effectively managed various types of technologies, including diverse distributed loads, ESSs, and RETs. While the DC MG considered DC loads, a WT, FC, an EZ, and an UC, the AC MG instead incorporated AC loads, BESS, and a PV generator.

The control system consisted in the use of local controllers for each device and a dynamic centralized optimal EMS, which coordinates power distribution with the objective of minimizing the power exchange with the local grid and ensuring a correct usage of the ESSs.

The control system and the MGC were tested under different operating scenarios. The simulation results demonstrated the robustness and effectiveness of the proposed control system and MGC. The system exhibited a satisfactory dynamic response, maintaining a minimal power exchange with the local grid remains minimal, thus fulfilling the primary optimization objective by using the ESSs efficiently. These findings highlight the potential of the proposed control system to enhance the efficiency and reliability of MGC.

While this paper provides valuable insights, future works could explore the impact of communication latencies and investigating the scalability of the control system for larger MGCs. Furthermore, experimental validation of the proposed control system could provide additional insights into its practical implementation.

Acknowledgement

This work was partially supported by Ministerio de Ciencia e Innovación, Agencia Estatal de Investigación, FEDER, UE (Grant PID2021-123633OB-C32 supported by MCIN/AEI/10.13039/501100011033/ FEDER, UE).

References

[1] E. Rosales-Asensio, D. B. Diez, P. Cabrera, and P. Sarmento, "Effectiveness and efficiency of support schemes in promoting renewable energy sources in the Spanish electricity market," *International Journal of Electrical Power & Energy Systems*, vol. 158, p. 109926, Jul. 2024, doi: 10.1016/J.IJEPES.2024.109926.

[2] A. Chebabhi, I. Tegani, A. D. Benhamadouche, and O. Kraa, "Optimal design and sizing of renewable energies in microgrids based on financial considerations a case study of Biskra, Algeria," *Energy Convers Manag*, vol. 291, p. 117270, Sep. 2023, doi: 10.1016/J.ENCONMAN.2023.117270.

[3] A. C. B. Monteiro, R. P. França, R. Arthur, and Y. Iano, "Overview of microgrids in the modern digital age: an introduction and fundamentals," *Residential Microgrids and Rural Electrifications*, pp. 27–43, Jan. 2022, doi: 10.1016/B978-0-323-90177-2.00011-6.

[4] R. Wang *et al.*, "Technology standards for direct current microgrids in buildings: A review," *Renewable and Sustainable Energy Reviews*, vol. 211, p. 115278, Apr. 2025, doi: 10.1016/J.RSER.2024.115278.

[5] Pragya and R. Thakur, "A Review of Architecture and Control Strategies of Hybrid AC/DC Microgrid," *2022 International Conference on Intelligent Controller and Computing for Smart Power, ICICCSP 2022*, 2022, doi: 10.1109/ICICCSP53532.2022.9862386.

[6] W. Dong *et al.*, "Stochastic optimal scheduling strategy for a campus-isolated microgrid energy management system considering dependencies," *Energy Convers Manag*, vol. 292, p. 117341, Sep. 2023, doi: 10.1016/J.ENCONMAN.2023.117341.

[7] G. Zhao, J. Luo, N. Song, and J. Shu, "Multi-objective optimal dispatch of island microgrid considering a novel scheduling resource," *Electric Power Systems Research*, vol. 241, p. 111378, Apr. 2025, doi: 10.1016/J.EPSR.2024.111378.

[8] A. Nawaz *et al.*, "MPC-driven optimal scheduling of grid-connected microgrid: Cost and degradation minimization with PEVs integration," *Electric Power Systems Research*, vol. 238, p. 111173, Jan. 2025, doi: 10.1016/J.EPSR.2024.111173.

[9] B. Chen, J. Wang, X. Lu, C. Chen, and S. Zhao, "Networked Microgrids for Grid Resilience, Robustness, and Efficiency: A Review," Jan. 01, 2021, *Institute of Electrical and Electronics Engineers Inc.* doi: 10.1109/TSG.2020.3010570.

[10] T. Sattarpour, S. Golshannavaz, D. Nazarpour, and P. Siano, "A multi-stage linearized interactive operation model of smart distribution grid with residential microgrids," *International Journal of Electrical Power & Energy Systems*, vol. 108, pp. 456–471, Jun. 2019, doi: 10.1016/J.IJEPES.2019.01.023.

[11] A. R. Abbasi and D. Baleanu, "Recent developments of energy management strategies in microgrids: An updated and comprehensive review and classification," *Energy Convers Manag*, vol. 297, p. 117723, Dec. 2023, doi: 10.1016/J.ENCONMAN.2023.117723.

[12] M. A. Hasan and S. K. Parida, "An overview of solar photovoltaic panel modeling based on analytical and experimental viewpoint," *Renewable and Sustainable Energy Reviews*, vol. 60, pp. 75–83, Jul. 2016, doi: 10.1016/J.RSER.2016.01.087.

[13] A. Yazdani and I. Reza, *Voltage source converter in power system*. 2010. Accessed: Jul. 28, 2023. [Online]. Available: https://www.wiley.com/en-ca/Voltage+Sourced+Converters+in+Power+Systems+%3A+Modeling%2C+Control%2C+and+Applications-p-9780470521564

[14] R. Sarrias-Mena, L. M. Fernández-Ramírez, C. A. García-Vázquez, and F. Jurado, "Electrolyzer models for hydrogen production from wind energy systems," *Int J Hydrogen Energy*, vol. 40, no. 7, pp. 2927–2938, Feb. 2015, doi: 10.1016/J.IJHYDENE.2014.12.125.

[15] F. Bandeiras, E. Pinheiro, M. Gomes, P. Coelho, and J. Fernandes, "Review of the cooperation and operation of microgrid clusters," Nov. 01, 2020, *Elsevier Ltd*. doi: 10.1016/j.rser.2020.110311.

.